JOURNAL OF VIROLOGY, Mar. 2005, p. 2743–2753 Vol. 79, No. 5
0022-538X/05/$08.00+0 doi:10.1128/JVI.79.5.2743–2753.2005

Nonstructural Protein σ1s Is a Determinant of Reovirus Virulence and Influences the Kinetics and Severity of Apoptosis Induction in the Heart and Central Nervous System

Cristen C. Hoyt,[1] Sarah M. Richardson-Burns,[2] Robin J. Goody,[3] Bridget A. Robinson,[3] Roberta L. DeBiasi,[3,4] and Kenneth L. Tyler[1,2,3,5,6,7]*

Departments of Immunology,[1] Neurology,[3] Pediatrics,[4] Microbiology,[5] and Medicine[6] and Program in Neurosciences,[2] University of Colorado Health Sciences Center, and Denver Veterans Affairs Medical Center,[7] Denver, Colorado

Received 25 May 2004/Accepted 11 October 2004

The mechanisms by which viruses kill susceptible cells in target organs and ultimately produce disease in the infected host remain poorly understood. Dependent upon the site of inoculation and strain of virus, experimental infection of neonatal mice with reoviruses can induce fatal encephalitis or myocarditis. Reovirus-induced apoptosis is a major mechanism of tissue injury, leading to disease development in both the brain and heart. In cultured cells, differences in the capacity of reovirus strains to induce apoptosis are determined by the S1 gene segment, which also plays a major role as a determinant of viral pathogenesis in both the heart and the central nervous system (CNS) in vivo. The S1 gene is bicistronic, encoding both the viral attachment protein sigma-1 and the nonstructural protein sigma-1-small (σ1s). Although σ1s is dispensable for viral replication in vitro, we wished to investigate the expression of σ1s in the infected heart and brain and its potential role in reovirus pathogenesis in vivo. Two-day-old mice were inoculated intramuscularly or intracerebrally with either $\sigma1s^-$ or $\sigma1s^+$ reovirus strains. While viral replication in target organs did not differ between $\sigma1s^-$ and $\sigma1s^+$ viral strains, virus-induced caspase-3 activation and resultant histological tissue injury in both the heart and brain were significantly reduced in $\sigma1s^-$ reovirus-infected animals. These results demonstrate that σ1s is a determinant of the magnitude and extent of reovirus-induced apoptosis in both the heart and CNS and thereby contributes to reovirus pathogenesis and virulence.

Experimental infection of neonatal mice with reovirus has provided important new insights into the mechanisms of viral entry, spread, tissue tropism, and disease pathogenesis in the infected host. Reoviruses infect and produce tissue injury in multiple organ systems, including the heart and central nervous system (CNS) (28, 31). Reovirus-induced apoptosis is a major mechanism of cell death, tissue injury, and ensuing disease in infected neonatal mice (8, 9, 19, 24, 25). In both the infected heart and brain, reovirus antigen, areas of histological injury, and apoptosis all colocalize (8, 19, 25). In the brain, type 3 (T3) reoviruses cause fatal encephalitis associated with neuronal injury and virus-induced apoptosis in neurons of the cortex, thalamus, and hippocampus (19, 24, 25). The viral S1 gene is a key determinant of the pattern of viral injury in the CNS (37, 38), although other viral genes play contributory roles as well (14). In the heart, reovirus-induced apoptosis appears to be the major mechanism for virus-induced myocardial injury and consequential death (8, 9). Reovirus genetics has identified multiple viral genes, including M1, L1, L2, and S1, as determinants of reovirus-induced acute myocarditis (28). S1 has been implicated as a major determinant of cytopathic effects in cardiomyocytes (3). The S1 gene is also a major determinant of differences in the capacity of reovirus strains to induce apoptosis in a variety of cultured cells (33, 34).

The S1 double-stranded RNA gene segment is bicistronic, encoding both the viral attachment protein sigma-1 (σ1) and the nonstructural protein sigma-1-small (σ1s) from overlapping but out-of-sequence open reading frames (11, 15, 27). σ1 is a structural protein located at the icosahedral vertices of the viral outer capsid and functions as the viral cell attachment protein (17). σ1 may influence virulence through its role in host cell receptor binding to mediate viral entry or through receptor-triggered intracellular signaling pathways (6, 20, 32). The second S1-encoded protein, σ1s, is a nonstructural protein and is a key determinant of the capacity of reoviruses to induce a G_2/M cell cycle arrest in infected cells (22, 23). We have recently shown that σ1s contains a functional nuclear localization signal and undergoes active signal-mediated nuclear import in both transfected and infected cells, resulting in profound disruption of nuclear architecture (13). Although a σ1s-null mutant replicates as well as wild-type T3 reovirus in cultured L929 and MDCK cells (26), the fact that σ1s is conserved in all known reovirus field isolates (5, 10) suggests that it plays an important role during viral pathogenesis in vivo. In order to evaluate the potential role of σ1s during pathogenesis, we compared heart and CNS disease following infection of neonatal mice with a σ1s-null reovirus mutant (C84-MA) to that following infection with σ1s-positive control strains.

We show that a σ1s deficiency does not affect viral growth in target tissues but profoundly reduces the capacity of reovirus to induce apoptosis and tissue injury in both the heart and the CNS. These studies indicate that although σ1s may not be

* Corresponding author. Mailing address: Department of Neurology (B-182), University of Colorado Health Sciences Center, 4200 E. 9th Ave., Denver, CO 80262. Phone: (303) 393-2874. Fax: (303) 393-4686. E-mail: Ken.Tyler@uchsc.edu.

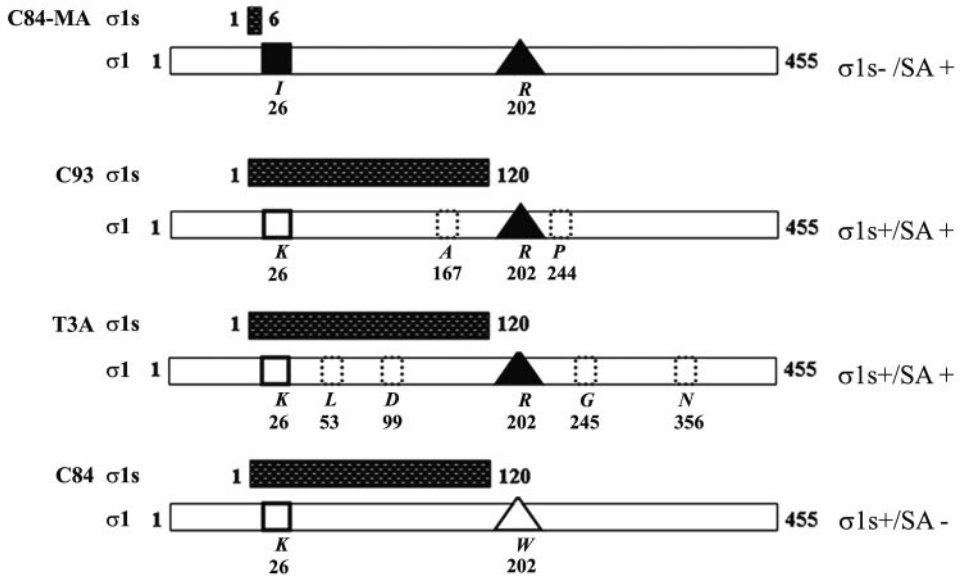

FIG. 1. $\sigma1s^-$ and $\sigma1s^+$ T3 reoviruses used in this study. Shown are representations of the 120-amino-acid σ1s protein sequence (stippled bars) and the 455-amino-acid σ1 protein sequence (white bars) for each viral strain used. C84-MA does not express σ1s due to an S1 gene mutation (black square). C84-MA, C93, and T3A bind SA (black triangles). C84 does not bind SA due to a mutation in σ1 (open triangle). C93 and T3A contain differences in the σ1 protein sequence compared to C84-MA (dotted boxes). Noted to the right is the σ1s expression status and SA binding ability of each strain.

required for viral replication in cultured cells, it plays a major role in viral virulence and disease outcome in vivo.

MATERIALS AND METHODS

Mice. Swiss-Webster mouse litters were housed in individual filter-topped cages in an American Association for Laboratory Animal Care-accredited animal facility. All animal procedures were performed under protocols approved by the appropriate institutional animal care and use committees.

Mouse inoculations. Two-day-old Swiss-Webster mice (Harlan Sprague-Dawley, Indianapolis, Ind.) were inoculated either intramuscularly (hind limb) or intracranially (right cerebral hemisphere) with 10^5 or 10^3 PFU (as specified) of the indicated reovirus strain in a 20-μl (intramuscular inoculation) or 10-μl (intracranial inoculation) volume of gel saline (137 mM NaCl, 0.2 mM $CaCl_2$, 0.8 mM $MgCl_2$, 19 mM H_3BO_3, 0.1 mM $Na_2B_4O_7$, 0.3% gelatin).

Viruses. The σ1s and σ1 protein sequences of the viruses used are diagrammed in Fig. 1. All viruses utilized were from laboratory stocks. T3C84 and T3C84-MA were originally provided by T. Dermody (Vanderbilt University, Nashville, Tenn.). T3 C84-MA is a σ1s-null mutant that was originally isolated following serial passage of the T3C84 (C84) strain through murine erythroleukemia cells (26). C84-MA contains a tryptophan (W)-to-arginine (R) mutation at position 202 which enables it to bind terminal sialic acid (SA) on glycosylated cellular proteins (SA^+), whereas C84 cannot (SA^-) (Fig. 1). C84-MA also contains an S1 gene mutation which results in a lysine (K)-to-isoleucine (I) substitution at amino acid 26 in σ1 (Fig. 1). This mutation also introduces a premature stop codon in σ1s. Since SA binding plays a significant role in reovirus pathogenesis (1, 2, 7), we used reovirus T3 clone 93 (C93) and the prototype T3 reovirus strain Abney (T3A), both of which bind SA, as additional controls for C84-MA. C93 expresses σ1s, binds SA coreceptors, and is the most closely related SA^+ field isolate to C84-MA in terms of its σ1 amino acid sequence. T3A expresses σ1s and binds to SA residues on target cells (Fig. 1).

Viral titer. Mice were sacrificed at the indicated times postinfection, and whole hearts or brains were placed in gel saline and immediately frozen at −70°C. After three freeze (−70°C)-thaw (37°C) cycles, tissues were sonicated for 30 s with a microtip probe (Heat Systems model XL2020) until a homogenate solution was formed. Viral suspensions were serially diluted in gel saline in 10-fold steps. Monolayers of L929 cells were infected with diluted virus in duplicate for plaque assay as previously described (36).

Histological analysis. Mice were sacrificed at the indicated times postinfection, and individual organs were immediately immersed in 10% buffered formalin solution for 24 h and then transferred to 70% ethanol for histological preparation. For the brain, paraffin-embedded tissues were cut to 4-μm coronal sections, showing cingulate cortex, frontoparietal cortex, hippocampus, and thalamus. Sections were stained with hematoxylin and eosin (H&E) for analysis of tissue pathology and quantitative scoring. Scoring of the extent of neuropathologic damage was based on a previously validated blinded grading system in which the extent of morphological changes and the area affected within specific brain regions were graded on a scale of 0 to 4 (30) (Table 1). For the heart, paraffin-embedded tissues were transversely cut to 4-μm sections. Quantitative scoring of histological injury in the heart was based on a previously validated blinded grading system in which the number and size of specific heart lesions were evaluated on a scale of 0 to 4 (8, 29) (Table 1). Histological injury in both the heart and brain was evaluated and scored from either a single coronal H&E-stained section per mouse or a single H&E-stained transverse heart section per mouse from multiple animals. For caspase-3 immunohistochemistry, 4-μm paraffin-embedded tissue sections were retrieved in a decloaker (BioCare, Vista, Calif.) in citrate buffer, followed by staining with rabbit anti-mouse polyclonal antibody directed against activated caspase-3 (Cell Signaling Technologies, Beverly, Mass.) at a 1:25 dilution, followed by detection by using an automated staining system with the Ventana (Tucson Ariz.) detection system. Quantitative scoring of caspase-3-stained tissue sections was based on a blinded grading system in which the number of caspase-3-positive cells and the size of caspase-3-positive areas were graded on a scale of 0 to 3 (Table 1). For σ1s immunohistochemistry in the brain, 4-μm paraffin-embedded coronal tissue sections were deparaffinized and retrieved in antigen-unmasking solution (Vector Laboratories, Burlingame, Calif.) according to the high-temperature unmasking technique provided by the manufacturer. After an overnight permeabilization with Neuropore at 4°C (Trevigen, Gaithersburg, Md.), goat anti-mouse monoclonal antibody directed against σ1s (3E2) was used at 200 μg/ml diluted into 3% bovine serum albumin (BSA)–Tris-buffered saline (TBS) plus 0.1% Tween (TBST) overnight at 4°C. As a secondary antibody, biotinylated goat anti-mouse antibody (Vector Laboratories) was used at 1:100 in 3% BSA–TBST for 2 h at 25°C. Detection was monitored by a diaminobenzidine tetrahydrochloride-based immunohistochemistry protocol according to the suggestions of the manufacturer (Vector Laboratories). Dehydration was carried out in a series of graded ethanol solutions, followed by clarification in xylene. Slides were mounted with

TABLE 1. Tissue section grading systems for apoptosis and histopathological damage in $\sigma1s^-$ and $\sigma1s^+$ reovirus-infected animals

Condition scored	Criteria for score of:				
	0	1	2	3	4
Apoptosis (CNS and heart)	No caspase-3-positive cells in tissue area	Scattered caspase-3-positive cells in tissue area	Groups of caspase-3-positive cells occupying up to 30% of affected tissue area	Groups of caspase-3-positive cells found in >30% of affected tissue area	
CNS histopathology[a]	No lesions	Affected area ≤10% of total section with morphological changes of individual dead neurons and small patchy areas of tissue destruction	Affected area approximately 10–40% of total section with partly confluent areas of tissue destruction	Affected area approximately 40–75% of total section with large confluent areas of tissue destruction	Affected area >75% of total section with total disintegration of cortical tissue, large complete areas of tissue destruction in the thalamus, and neuronal death in the hippocampus
Cardiac histopathology[b]	No lesions	One or a few small lesions	Many small or a few large lesions	Multiple small and large lesions	Massive lesions

[a] As described in reference 30.
[b] As described in references 8 and 29.

Vectamount (Vector Laboratories) and stored at 25°C. A similar procedure was used to evaluate σ1s expression in cardiac tissue sections, with the following exceptions: monoclonal antibody 2F4 was used as the primary antibody at a concentration of 100 μg/ml, diluted into 3% BSA–TBST, overnight at 4°C. The hybridoma cell lines synthesizing the anti-σ1s antibodies, 2F4 and 3E2, were generous gifts (26). Anti-σ1s antibodies were purified on protein A columns based on the recommended protocol described by the manufacturer (Pierce, Rockford, Ill.). For reovirus antigen detection (reovirus structural proteins), deparaffinized tissue sections were retrieved in antigen-unmasking solution (Vector Laboratories) according to the high-temperature unmasking technique provided by the manufacturer and permeabilized in Neuropore (Trevigen) at 4°C overnight. Rabbit polyclonal reovirus antiserum was used at 1:200 in 5% normal goat serum–TBST at 25°C for 1 h. Extensive washing in TBST was followed by incubation in fluorescein isothiocyanate-conjugated goat anti-rabbit immunoglobulin G (Vector Laboratories) diluted at 1:100 in 3% BSA–TBST. After extensive washing in TBST and TBS, nuclei were visualized with Hoechst 33342 (Molecular Probes, Eugene, Oreg.). Stained sections were mounted with Vectashield (Vector Laboratories) and stored at 4°C.

Statistics. All statistical analyses were performed with In Stat version 3.0 (Graph Pad, San Diego, Calif.).

RESULTS

σ1s enhances reovirus virulence following intramuscular inoculation. In order to evaluate the role of σ1s in the induction of reovirus-induced myocarditis, 2-day-old neonatal mice were inoculated intramuscularly with 10^5 PFU of reovirus strain C84-MA ($\sigma1s^-$ SA^+), C93 ($\sigma1s^+$ SA^+), T3A ($\sigma1s^+$ SA^+), or C84 ($\sigma1s^+$ SA^-). Infected animals were examined daily to assess health and progression of disease (Fig. 2). All C84-MA ($\sigma1s^-$ SA^+)-infected mice survived virus challenge, whereas all mice infected with the control T3A ($\sigma1s^+$ SA^+) or C93 ($\sigma1s^+$ SA^+) strain appeared to be sick at approximately 6 days postinfection and died within 14 days of infection (mean day of death ± standard error of the mean, 9.9 ± 1.2 days or 10.4 ± 0.5, respectively) (Fig. 2). The $\sigma1s^+$ SA^- strain C84 showed an intermediate phenotype, with 30% mortality (Fig. 2). The observed differences in patterns of lethality between $\sigma1s^-$ and $\sigma1s^+$ strains indicated that σ1s was an important determinant of virulence following peripheral intramuscular inoculation. The intermediate phenotype of the SA^- strain C84 indicated that in addition to the presence or absence of σ1s, SA binding is likely to be an important determinant of reovirus virulence following intramuscular inoculation.

σ1s is not required for viral replication in the heart. Following intramuscular inoculation of either $\sigma1s^-$ or $\sigma1s^+$ reovirus strains, the viral titer in the hearts of infected animals was determined at 8 days postinfection. There were no significant differences in titer observed between virus strains in the heart ($P > 0.05$ for all interstrain comparisons) (Fig. 3). σ1s was therefore not required for either efficient spread to or growth within the heart. Similarly, no significant differences in titer were observed between SA^+ and SA^- viruses (Fig. 3), suggesting that SA binding was also not a significant determinant of

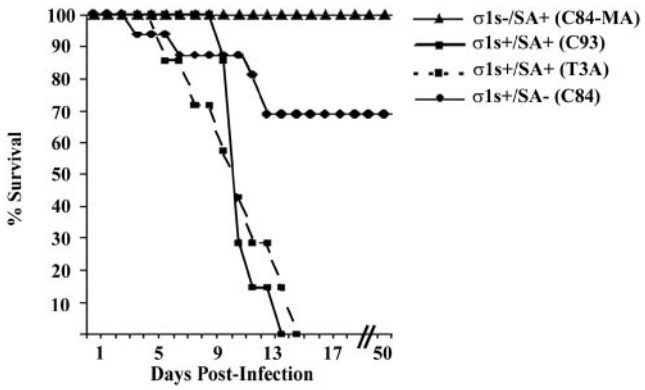

FIG. 2. σ1s confers enhanced virulence following intramuscular reovirus inoculation. Neonatal mice (n = 7 to 16) were inoculated intramuscularly with C84-MA ($\sigma1s^-$ SA^+), C93 ($\sigma1s^+$ SA^+), T3A ($\sigma1s^+$ SA^+), or C84 ($\sigma1s^+$ SA^-).

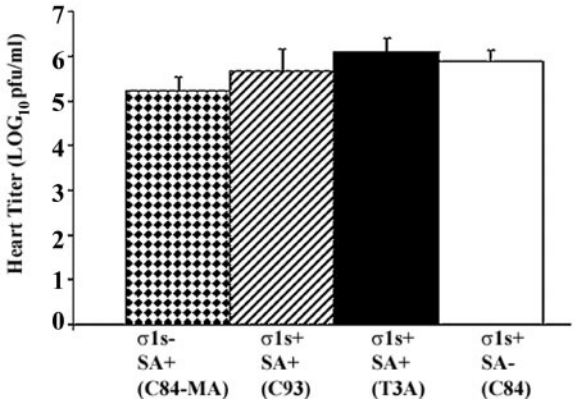

FIG. 3. σ1s does not influence viral growth in the heart. Viral titers in infected hearts were not significantly different ($P > 0.05$) between $\sigma1s^-$ and all $\sigma1s^+$ viral strains. Each bar represents the average viral titer from 5 to 10 mice at 8 days post-intramuscular inoculation. Error bars indicate standard errors of the means.

spread to or growth within the heart in infected animals following intramuscular peripheral inoculation.

σ1s is a determinant of apoptosis and pathogenesis in the heart. Having shown that σ1s is a determinant of lethality following intramuscular reovirus inoculation, we next determined the effect of σ1s on viral pathogenesis in hearts of reovirus-infected animals. To evaluate overall myocardial tissue injury, H&E-stained transverse cardiac sections were evaluated via light microscopy, and the degree of injury was quantified by using a previously validated scoring system (8, 29) (Table 1 and Fig. 4). At 8 days postinfection, prominent myocardial disruption, numerous apoptotic bodies, and evidence of pyknotic nuclei were observed in hearts of $\sigma1s^+$ virus-infected mice regardless of SA binding ability, while very minor myocardial injury was noted in $\sigma1s^-$ reovirus-infected animals (Fig. 4).

Immunohistochemical detection of the activated form of caspase-3 was used as a marker of apoptosis in reovirus-infected hearts. Dark brown staining indicates active caspase-3 apoptotic lesions within the myocardium (Fig. 5B and C). Mice infected with the $\sigma1s^-$ strain C84-MA showed a significant decrease in both the number and size of apoptotic lesions in the heart compared to each of the $\sigma1s^+$ control viruses at 8 days postinfection (Fig. 5A). In contrast, all $\sigma1s^+$ reoviruses produced severe myocardial injury with extensive areas of apoptosis analogous to those we have previously described for the prototypic myocarditis-inducing strain, 8B (8). The rare apoptotic lesions that were observed in $\sigma1s^-$ virus-infected hearts appeared similar in cellular composition and caspase-3 staining to heart lesions seen in $\sigma1s^+$ virus-infected hearts (data not shown).

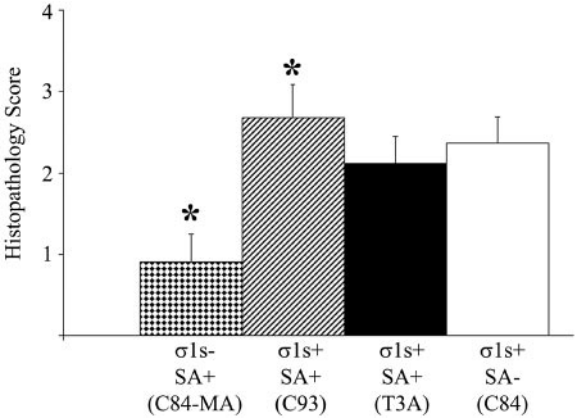

FIG. 4. σ1s is required for maximal myocardial tissue injury. The degree of injury in the myocardium, as measured by quantifying H&E-stained heart sections, was significantly reduced in $\sigma1s^-$ (C84-MA) virus-infected mice. Each bar represents the average score from 10 to 13 mice. Error bars indicate standard errors of the means. *, $P < 0.05$.

Animals which survived C84-MA ($\sigma1s^-$ SA^+) virus challenge were sacrificed at 50 days postinfection and evaluated for myocardial injury. H&E-stained heart sections did not show any myocarditic damage, and no infectious virus was detectable by plaque assay in the heart or other organs (data not shown).

Taken together, these studies indicate that σ1s was a determinant of the extent and severity of myocardial injury and apoptosis but not of viral growth in the hearts of infected mice. We next wished to determine whether these same features occurred in CNS infection.

σ1s is a determinant of T3 reovirus virulence following intracranial inoculation. In order to study the role of σ1s in pathogenesis of reovirus-induced CNS disease, 2-day-old mice were intracerebrally inoculated with 10^3 PFU of reovirus strain C84-MA ($\sigma1s^-$ SA^+), C93 ($\sigma1s^+$ SA^+), T3A ($\sigma1s^+$ SA^+), or C84 ($\sigma1s^+$ SA^-). Mortality was monitored for 30 days following inoculation (Fig. 6). One hundred percent of mice infected with either C93 or T3A died (mean day of death ± standard error of the mean, 9.1 ± 0.8 and 8.9 ± 0.3, respectively), compared to only 67% of C84-MA-infected mice (mean day of death ± standard error of the mean, 14.3 ± 1.2) ($P < 0.001$). The SA^- strain C84 also showed enhanced survival compared to T3A and C93 (Fig. 6).

In an effort to see whether the attenuated phenotype of C84-MA ($\sigma1s^-$ SA^+) would persist after massive viral challenge, mice were injected intracranially with 10^5 PFU (approximately 10,000 times the intracranial 50% lethal dose) of the test viruses per mouse. All mice died at this high challenge dose, although the mean day of death for $\sigma1s^-$ virus (C84-MA)-infected mice was significantly ($P < 0.001$) prolonged (11.2 ± 0.3 days) compared to that for either $\sigma1s^+$ T3A (8.3 ± 0.3 days)- or $\sigma1s^+$ C93 (9 ± 0 days)-infected animals.

These results indicate that σ1s is a determinant of neurovirulence following intracerebral inoculation of reovirus. The enhanced survival in mice infected with the SA^- strain C84 compared to the SA^+ strains T3A and C93 also indicate that SA binding plays a role in neurovirulence.

σ1s is not required for viral replication in the brain. Having shown that σ1s influenced neurovirulence after intracranial inoculation, we next wished to determine whether this was due to an effect on viral growth in the CNS. Neonatal mice were intracerebrally infected with 10^5 PFU of the various reovirus strains. At 8 days postinfection brain tissue was removed from euthanatized animals, and the viral titer was determined by plaque assay of brain homogenates (Fig. 7). As seen in the heart model, the presence or absence of σ1s did not significantly affect viral growth in the brain ($P > 0.05$ for all inter-

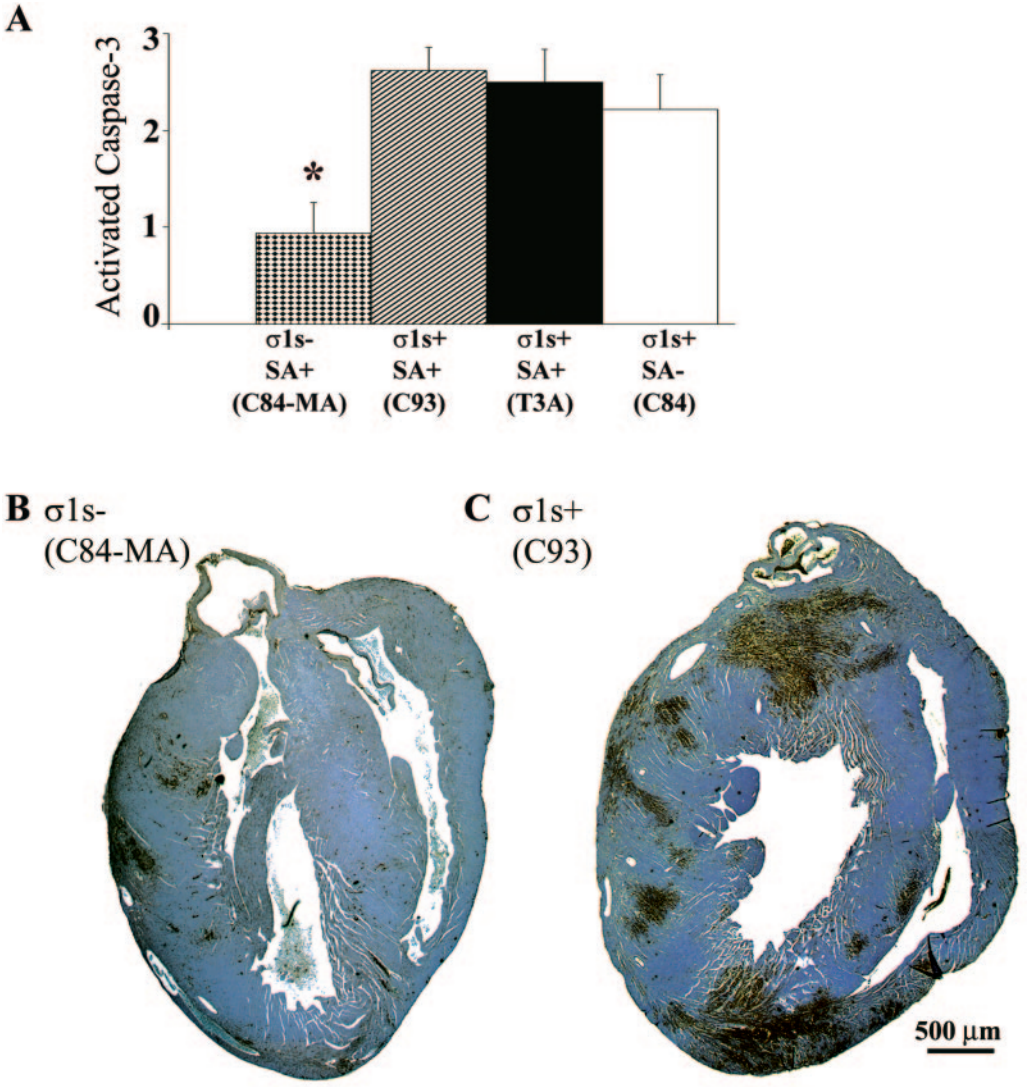

FIG. 5. σ1s is required for maximal apoptosis induction in the heart. Immunohistochemical staining of activated caspase-3 in whole hearts (B and C) (original magnification, ×25) demonstrates that loss of σ1s expression significantly reduces reovirus-induced apoptosis (A). In panel A, each bar represents the average score from four to eight mice. Error bars indicate standard errors of the means. *, $P < 0.05$.

strain comparisons except that between the SA^- virus C84 and the SA^+ virus T3A, for which $P < 0.01$). These results indicate that σ1s does not influence viral growth in the brain.

σ1s is a determinant of apoptosis and pathogenesis in the brain. We next wished to determine whether σ1s influenced the extent of viral injury in the CNS. At 8 days following infection, mice were sacrificed and neuropathologic injury was evaluated. The $\sigma1s^-$ strain C84-MA (Fig. 8A to C and J) induced significantly less tissue injury in the cortex, thalamus, and hippocampus than its $\sigma1s^+$ SA^+ counterparts (Fig. 8D to I and J). By contrast, large areas in the thalamus and cortex of $\sigma1s^+$ SA^+ (C93 and T3A) virus-infected animals were destroyed and contained numerous apoptotic bodies (Fig. 8D and E). Extensive neuronal death was also evident in the hippocampi of these animals (Fig. 8F). $\sigma1s^-$ (C84-MA) virus-infected mice, examined when moribund (day 11), did show substantial CNS injury (data not shown), indicating that loss of σ1s delayed but did not prevent the appearance of CNS injury following high-dose virus challenge. The SA^- virus (C84) also showed markedly reduced tissue injury (Fig. 8G to J) compared to SA^+ $\sigma1s^+$ virus C93 (Fig. 8D to F) or T3A (data not shown). When moribund, C84-infected mice displayed delayed CNS injury (data not shown).

Immunohistochemical detection of the activated form of caspase-3 was used as a marker for reovirus-induced apoptosis in the brain. Mice infected with $\sigma1s^-$ virus (C84-MA) had no detectable apoptosis in the cortex, thalamus, or hippocampus at 8 days postinfection (Fig. 9B). Conversely, $\sigma1s^+$ control strains C93 (Fig. 9D) and T3A (data not shown) displayed high levels of caspase-3 activation in all three areas. The SA^- virus C84 also displayed substantially reduced apoptosis in the cortex, thalamus, and hippocampus (Fig. 9C). As was the case for histological injury, C84-MA-infected mice examined when moribund (day 11) showed substantial caspase-3 activation

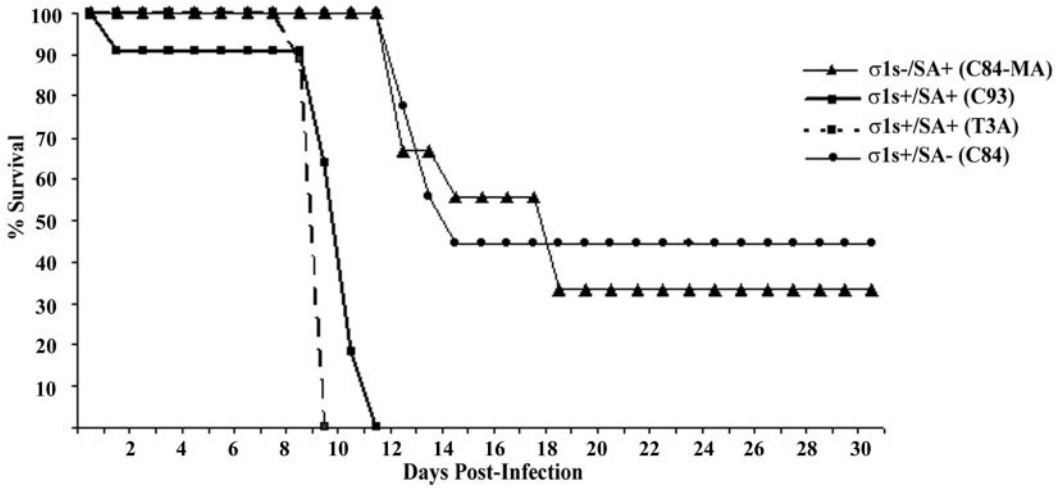

FIG. 6. σ1s confers enhanced virulence following intracranial inoculation. Neonatal mice (n = 7 to 11) were inoculated intracerebrally with 10^3 PFU of C84-MA ($\sigma1s^-$ SA^+), C93 ($\sigma1s^+$ SA^+), T3A ($\sigma1s^+$ SA^+), or C84 ($\sigma1s^+$ SA^-) per mouse.

(data not shown), indicating that loss of σ1s served to delay but not prevent apoptosis following high-dose viral challenge.

By contrast to the results seen following high-dose viral challenge, long-term survivors of low-dose intracerebral challenge with $\sigma1s^-$ reovirus (Fig. 6) sacrificed at 30 days postinfection did not show any histopathological indication of viral damage, and no infectious virus was detectable by plaque assay in the brain or other organs (data not shown). Similar results were obtained with survivors of SA^- (C84) infection as well (data not shown).

Expression of σ1s in vivo by reovirus strains. We next wished to evaluate σ1s expression by C84-MA ($\sigma1s^-$ SA^+) and the $\sigma1s^+$ strains T3A, C93, and C84 following both intramuscular (Fig. 10A to F) and intracranial (Fig. 10G to L) inoculation of neonatal mice. In vivo σ1s expression was evaluated by staining cardiac and coronal sections from $\sigma1s^-$ and $\sigma1s^+$ virus-infected animals with monoclonal antibodies directed against T3 σ1s. Expression of reovirus structural proteins was evaluated by using polyclonal antisera in adjacent sections.

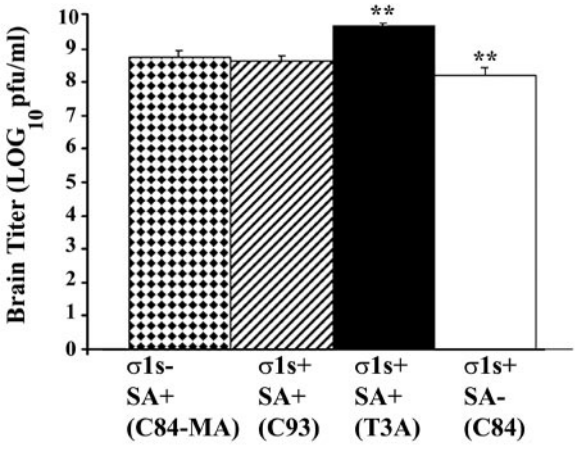

FIG. 7. σ1s does not influence viral growth in the brain. Viral titers were not significantly different between $\sigma1s^-$ and all $\sigma1s^+$ viral strains ($P > 0.05$). T3A and C84 viral titers were significantly different (**, $P < 0.01$). Each bar represents the average viral titer from three to six mice 8 days post-intracranial inoculation. Error bars indicate standard errors of the means.

As expected, both heart and brain tissues from C84-MA ($\sigma1s^-$ SA^+)-infected mice did not show positive σ1s staining (Fig. 10C and I) despite detectable expression of reovirus structural proteins (Fig. 10F and L). These data indicate that reovirus was present in both the infected hearts and brains of C84-MA mice but was not expressing σ1s.

In contrast, coronal sections from $\sigma1s^+$ SA^+ (T3A) virus-infected mice displayed prominent expression of σ1s (Fig. 10G) and structural proteins (Fig. 10J) within the cortex, as well as the thalamus and hippocampus (data not shown). In the heart, the $\sigma1s^+$ strain T3A displayed high levels of σ1s staining (Fig. 10A) and structural proteins (Fig. 10D) within areas of cardiac lesions. The $\sigma1s^+$ SA^+ strain C93 displayed staining patterns similar to those of T3A in both the heart and brain (data not shown). In contrast to the exclusively cytoplasmic localization of reovirus structural proteins in infected cardiomyocyte neurons, σ1s was observed in both the cytoplasm and nuclei of infected cells, thus corroborating in vivo our previous in vitro data indicating that σ1s localizes to both the cytoplasm and nuclei of infected cells (13).

The $\sigma1s^+$ SA^- strain C84 expressed σ1s in both the heart and CNS (Fig. 10B and H). In the brain, reovirus structural proteins were observed throughout the cortex (Fig. 10K), thalamus (data not shown), and hippocampus (data not shown). The relative amount of σ1s expression compared to structural protein expression appeared to be lower in C84-infected mice than in T3A- or C93-infected mice, particularly in the CNS (Fig. 10G, J, H, and K). In the heart, the ratio of σ1s expression to expression of reovirus structural proteins seemed to approximate that for T3A (Fig. 10 A, D, B, and E). Although these data are not quantitative, the reduced level of σ1s expression compared to that of reovirus structural protein expression observed in C84 infected tissues suggests that C84 may express σ1s at reduced levels compared to $\sigma1s^+$ SA^+ strains, a result also noted in vitro (26).

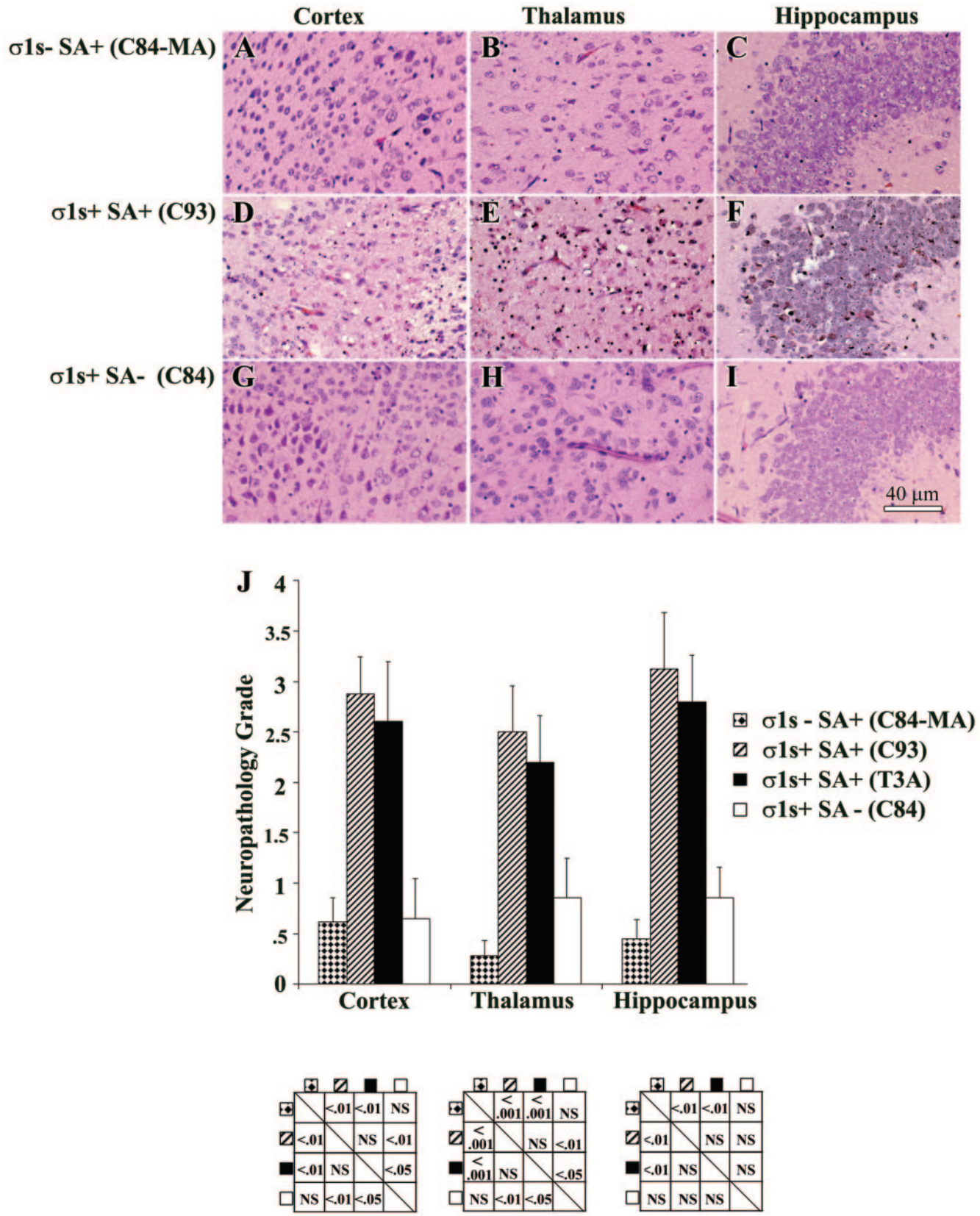

FIG. 8. σ1s determines the extent and severity of reovirus-induced CNS injury. Representative H&E-stained coronal sections of the cortex, thalamus, and hippocampus are shown for C84-MA (A to C), C93 (D to F), and C84 (G to I) (original magnification, ×400). Tissue injury was quantified by using a previously validated neuropathology grading system (J). Each bar represents the average score from four to nine mice. Error bars indicate standard errors of the means. Statistical comparisons are shown in below the corresponding areas of the graph. NS, not significant.

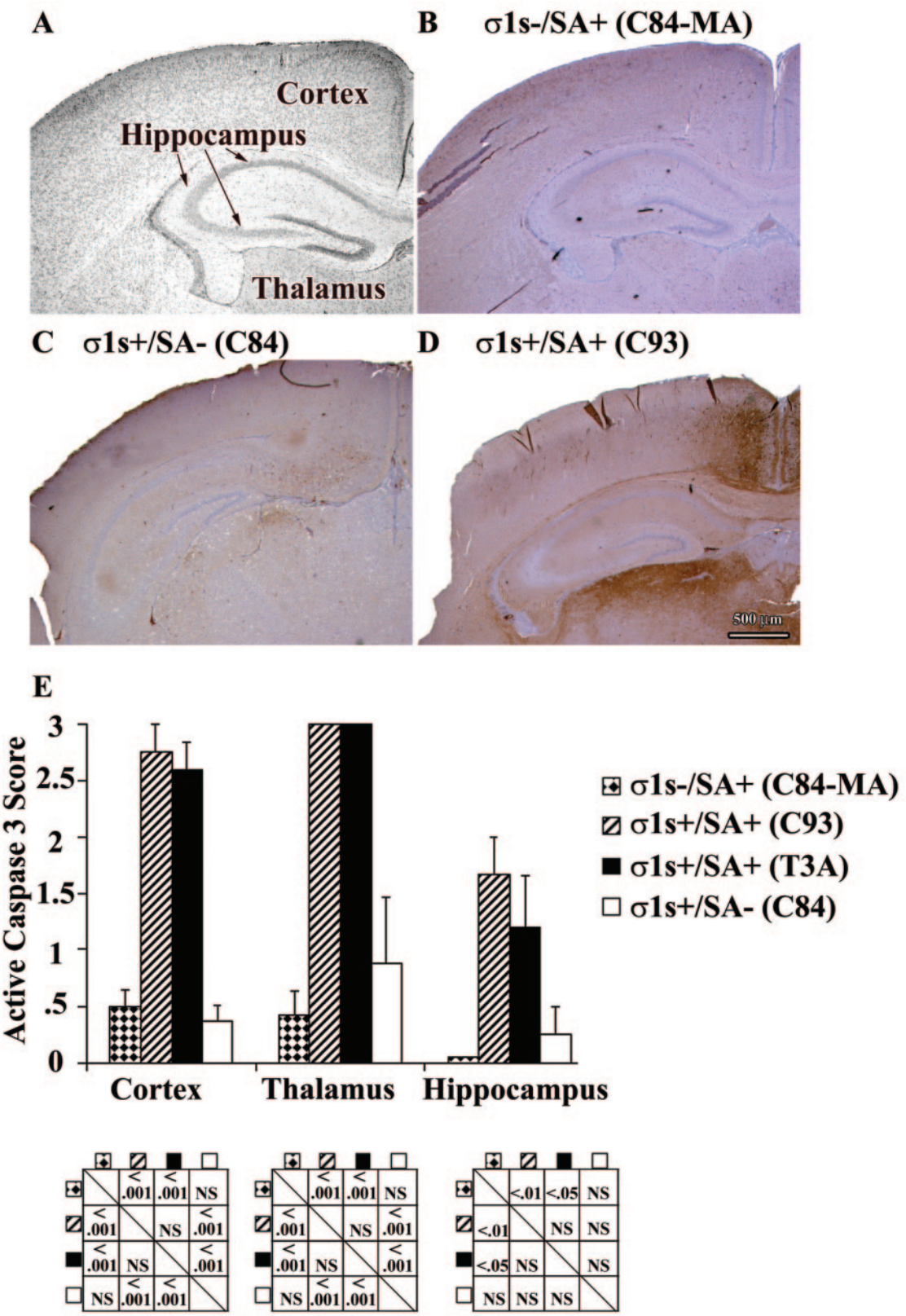

FIG. 9. σ1s determines the extent and severity of reovirus-induced apoptosis in the brain. The cortex, hippocampus, and thalamus were examined at 8 days post-intracranial inoculation (A). Active, cleaved caspase-3 was quantified by the number and size of caspase-3-positive apoptotic areas (E). C84-MA ($\sigma1s^{-}$ SA^{+})-infected mice displayed reduced caspase-3 activation in the brain compared to $\sigma1s^{+}$ control viruses (B to E) (original magnification, ×25). In panel E, each bar represents the average score from four to seven mice. Error bars indicate standard errors of the means. Statistical comparisons are shown in below the corresponding areas of the graph. NS, not significant.

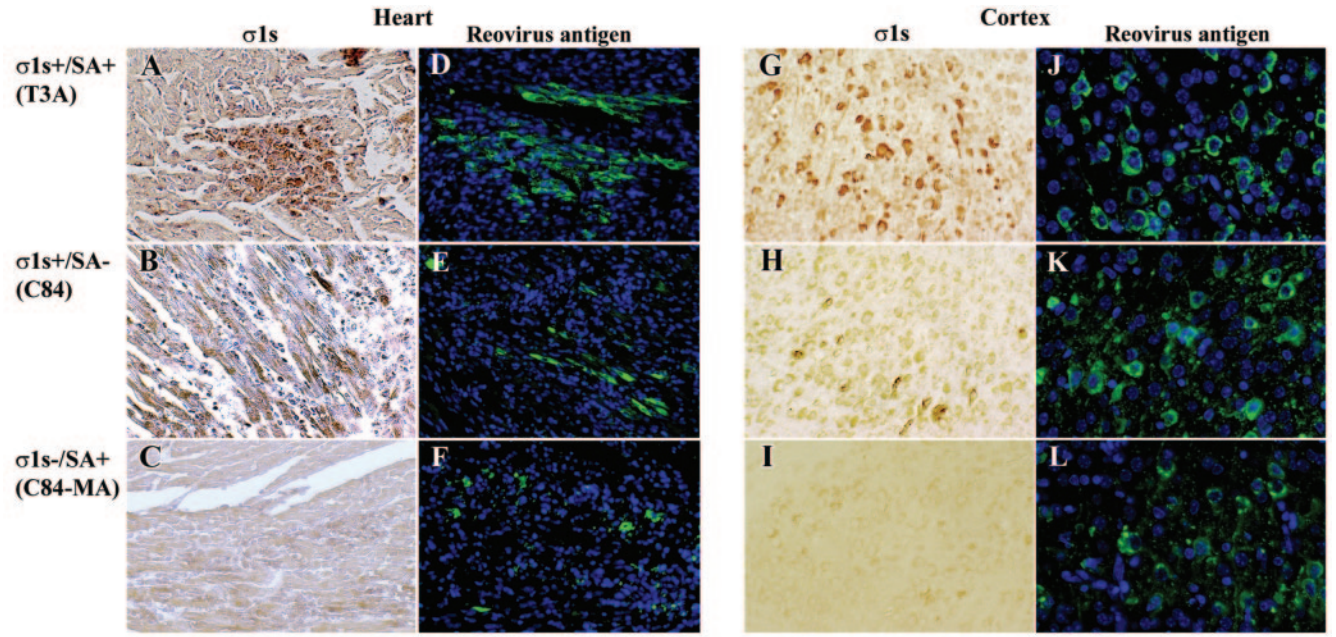

FIG. 10. σ1s is expressed in vivo following both intramuscular and intracranial inoculation with 10^5 PFU of T3A ($\sigma1s^+$ SA^+) (A and G) and C84 ($\sigma1s^+$ SA^-) (B and H), but not C84-MA ($\sigma1s^-$ SA^+) (C and I), per mouse. In vivo σ1s expression in both the hearts and brains of infected animals was evaluated by diaminobenzidine tetrahydrochloride immunohistochemistry with monoclonal antibodies specific for T3 σ1s. Cardiac sections from intramuscularly inoculated mice (T3A, C84, and C84-MA) were stained with monoclonal antibody 2F4 directed against σ1s (A to C) (original magnification, ×200) and polyclonal antisera directed against reovirus structural proteins (D to F) (original magnification, ×100). Coronal sections from intracranially inoculated mice (T3A, C84, and C84-MA) were stained with monoclonal antibody 3E2 directed against σ1s (G to I) (original magnification, ×200) and polyclonal antisera directed against reovirus structural proteins (J to L) (original magnification, ×400). Polyclonal antiserum directed against T3 reovirus structural proteins was used as a control for the presence of reovirus in both cardiac (D to F) and brain (J to L) tissues.

DISCUSSION

We now show that the reovirus nonstructural σ1s protein is a determinant of viral injury in the hearts and brains of infected neonatal mice. Although viral growth in the brain and heart was not affected by the presence or absence of σ1s, the extent of reovirus-induced apoptosis induction and severity of ensuing tissue damage in both organs was significantly influenced by σ1s expression. In addition, $\sigma1s^-$ SA^+ (C84-MA) virus-infected animals displayed enhanced survival following either intramuscular or intracranial challenge compared to mice injected with $\sigma1s^+$ SA^+ viral strains. These studies provide the first demonstration that σ1s is expressed following intramuscular or intracranial inoculation and plays a significant role in reovirus pathogenesis in vivo.

Our results demonstrate that σ1s expression does not influence viral growth in the heart or brain and supports previous in vitro data indicating that σ1s is not required for reovirus replication in either L929 or MDCK cells (26). We further demonstrate that σ1s influences the rate and extent of apoptosis induction in vivo, a phenomenon not obvious in vitro (26). This is not surprising, as there are many host factors that may operate in concert with σ1s or other reovirus proteins to affect reovirus-induced disease in vivo (35). For example, σ1s elicits a strong and specific cytotoxic-T-lymphocyte response (12) which may contribute to the ability of σ1s to modulate the extent and severity of apoptosis induction that we observed in vivo. The conservation of σ1s open reading frames in all reovirus field isolates provides further support for the conclusion that σ1s plays an important role during viral pathogenesis in vivo.

We have recently shown that σ1s actively localizes to the nucleus in infected cells and induces severe disruptions in nuclear architecture, including perturbation of the A-type nuclear lamina network (LaA/C) and induction of nuclear herniations (13). The relationship, if any, between σ1s-induced nuclear architecture changes observed in vitro and the described effects on pathogenesis in vivo are unknown. However, recent studies report that disruption of LaA/C in myocardiocytes weakens nuclear structural mechanics and renders cells more sensitive to apoptosis following mechanical stress, such as that generated by the beating myocardium (16). This suggests the possibility that σ1s-induced LaA/C defects may also function in vivo to render infected myocardiocytes more susceptible to apoptosis induction by reovirus.

The apoptosis-enhancing effects of LaA/C disruption are less likely the potential mechanism of action for σ1s in the CNS due to the lack of mechanical strain in brain tissue. Other cytopathic effects of σ1s may possibly influence the extent and severity of apoptosis induction in the brain. A growing body of evidence suggests that aberrant reentry into the cell cycle or abnormal expression of key cell cycle regulatory proteins represents a common mechanism of neuronal apoptosis (4). σ1s modulates induction of reovirus-induced G_2/M cell cycle arrest in infected cells and inhibits p34 (cdc2) kinase activity (22). In

addition, reovirus infection alters the expression profiles of key cell cycle proteins (21). Given these data, it is plausible that in reovirus-infected neurons, σ1s perturbation of cell cycle regulatory proteins may exacerbate reovirus-induced neuronal apoptosis.

SA binding optimizes induction of apoptosis in a variety of cultured cells (7, 20) and is required for full expression of certain disease phenotypes, including reovirus-induced biliary atresia (2). Our studies suggest that SA binding is not essential for reovirus spread to and growth within the heart following peripheral inoculation. SA binding is not required for apoptosis induction in the heart or development of myocarditis, as the SA^- strain (C84) was efficiently myocarditic and induced apoptosis. SA binding may be more important in CNS pathogenesis than in the heart, as the SA^- strain (C84) showed reduced CNS tissue injury and apoptosis compared to the control $\sigma1s^+$ SA^+ strains (T3A and C93).

An additional factor that may influence pathogenesis is differences in the amount of σ1s expression in vivo. C84-MA ($\sigma1s^-$ SA^+) does not express σ1s in vivo and is significantly less pathogenic in both the heart and the CNS. The SA^- strain C84 also appeared to have lower levels of σ1s expression in vivo than other $\sigma1s^+$ strains. Although not quantitative, our data support previous in vitro data (26) and suggest that the altered phenotype of C84 could also reflect reduced σ1s expression.

Our findings represent the first evidence of a role for the nonstructural reovirus protein σ1s in viral pathogenesis in vivo. The onset of apoptosis induction and severity of virus-induced tissue injury are both dependent on the expression of σ1s. The evidence presented here is all the more provocative considering the implication of a role for σ1s in virus-induced pathogenesis independent of any effects on viral growth.

ACKNOWLEDGMENTS

This work was supported by Merit and REAP grants from the Department of Veterans Affairs NIH NINDS 1ROINS50138 (to K.L.T.), U.S. Army Medical Research and Material Command grant DAMD17-98-1-8614 (to K.L.T.), and the Reuler-Lewin Family Professorship of Neurology (to K.L.T.).

We acknowledge the University of Colorado Health Sciences Center Histology Services for assisting with histological preparation.

REFERENCES

1. **Barton, E. S., J. L. Connolly, J. C. Forrest, J. D. Chappell, and T. S. Dermody.** 2001. Utilization of sialic acid as a coreceptor enhances reovirus attachment by multistep adhesion strengthening. J. Biol. Chem. **276:**2200–2211.
2. **Barton, E. S., B. E. Youree, D. H. Ebert, J. C. Forrest, J. L. Connolly, T. Valyi-Nagy, K. Washington, J. D. Wetzel, and T. S. Dermody.** 2003. Utilization of sialic acid as a coreceptor is required for reovirus-induced biliary disease. J. Clin. Investig. **111:**1823–1833.
3. **Baty, C. J., and B. Sherry.** 1993. Cytopathogenic effect in cardiac myocytes but not in cardiac fibroblasts is correlated with reovirus-induced acute myocarditis. J. Virol. **67:**6295–6298.
4. **Becker, E. B., and A. Bonni.** 2004. Cell cycle regulation of neuronal apoptosis in development and disease. Prog. Neurobiol. **72:**1–25.
5. **Cashdollar, L. W., R. A. Chmelo, J. R. Wiener, and W. K. Joklik.** 1985. Sequences of the S1 genes of the three serotypes of reovirus. Proc. Natl. Acad. Sci. USA **82:**24–28.
6. **Clarke, P., and K. L. Tyler.** 2003. Reovirus-induced apoptosis. Apoptosis **8:**141–150.
7. **Connolly, J. L., E. S. Barton, and T. S. Dermody.** 2001. Reovirus binding to cell surface sialic acid potentiates virus-induced apoptosis. J. Virol. **75:**4029–4039.
8. **DeBiasi, R. L., C. L. Edelstein, B. Sherry, and K. L. Tyler.** 2001. Calpain inhibition protects against virus-induced apoptotic myocardial injury. J. Virol. **75:**351–361.
9. **DeBiasi, R. L., B. A. Robinson, B. Sherry, R. Bouchard, R. D. Brown, M. Rizeq, C. Long, and K. L. Tyler.** 2004. Caspase inhibition is protective against reovirus-induced myocardial injury in vitro and in vivo. J. Virol. **78:**11040–11050.
10. **Dermody, T. S., M. L. Nibert, R. Bassel-Duby, and B. N. Fields.** 1990. Sequence diversity in S1 genes and S1 translation products of 11 serotype 3 reovirus strains. J. Virol. **64:**4842–4850.
11. **Ernst, H., and A. J. Shatkin.** 1985. Reovirus hemagglutinin mRNA codes for two polypeptides in overlapping reading frames. Proc. Natl. Acad. Sci. USA **82:**48–52.
12. **Hoffman, L. M., K. T. Hogan, and L. W. Cashdollar.** 1996. The reovirus nonstructural protein σ1NS is recognized by murine cytotoxic T lymphocytes. J. Virol. **70:**8160–8164.
13. **Hoyt, C. C., R. J. Bouchard, and K. L. Tyler.** 2004. Novel nuclear herniations induced by nuclear localization of a viral protein. J. Virol. **78:**6360–6369.
14. **Hrdy, D. B., D. H. Rubin, and B. N. Fields.** 1982. Molecular basis of reovirus neurovirulence: role of the M2 gene in avirulence. Proc. Natl. Acad. Sci. USA **79:**1298–1302.
15. **Jacobs, B. L., and C. E. Samuel.** 1985. Biosynthesis of reovirus-specified polypeptides: the reovirus s1 mRNA encodes two primary translation products. Virology **143:**63–74.
16. **Lammerding, J., P. C. Schulze, T. Takahashi, S. Kozlov, T. Sullivan, R. D. Kamm, C. L. Stewart, and R. T. Lee.** 2004. Lamin A/C deficiency causes defective nuclear mechanics and mechanotransduction. J. Clin. Investig. **113:**370–378.
17. **Nibert, M. L., and L. A. Schiff.** 2001. Reoviruses and their replication, p. 793–842. *In* D. M. Knipe and P. M. Howley (ed.), Fundamental virology. Lippincott Williams & Wilkins, Philadelphia, Pa.
18. **Oberhaus, S. M., T. S. Dermody, and K. L. Tyler.** 1998. Apoptosis and the cytopathic effects of reovirus. Curr. Top. Microbiol. Immunol. **233:**23–49.
19. **Oberhaus, S. M., R. L. Smith, G. H. Clayton, T. S. Dermody, and K. L. Tyler.** 1997. Reovirus infection and tissue injury in the mouse central nervous system are associated with apoptosis. J. Virol. **71:**2100–2106.
20. **O'Donnell, S. M., M. W. Hansberger, and T. S. Dermody.** 2003. Viral and cellular determinants of apoptosis induced by mammalian reovirus. Int. Rev. Immunol. **22:**477–503.
21. **Poggioli, G. J., R. L. DeBiasi, R. Bickel, R. Jotte, A. Spalding, G. L. Johnson, and K. L. Tyler.** 2002. Reovirus-induced alterations in gene expression related to cell cycle regulation. J. Virol. **76:**2585–2594.
22. **Poggioli, G. J., T. S. Dermody, and K. L. Tyler.** 2001. Reovirus-induced σ1s-dependent $G_{(2)}$/M phase cell cycle arrest is associated with inhibition of p34 (cdc2). J. Virol. **75:**7429–7434.
23. **Poggioli, G. J., C. Keefer, J. L. Connolly, T. S. Dermody, and K. L. Tyler.** 2000. Reovirus-induced $G_{(2)}$/M cell cycle arrest requires σ1s and occurs in the absence of apoptosis. J. Virol. **74:**9562–9570.
24. **Richardson-Burns, S. M., D. J. Kominsky, and K. L. Tyler.** 2002. Reovirus-induced neuronal apoptosis is mediated by caspase 3 and is associated with the activation of death receptors. J. Neurovirol. **8:**365–380.
25. **Richardson-Burns, S. M., and K. L. Tyler.** 2004. Regional differences in viral growth and central nervous system injury correlate with apoptosis. J. Virol. **78:**5466–5475.
26. **Rodgers, S. E., J. L. Connolly, J. D. Chappell, and T. S. Dermody.** 1998. Reovirus growth in cell culture does not require the full complement of viral proteins: identification of a σ1s-null mutant. J. Virol. **72:**8597–8604.
27. **Sarkar, G., J. Pelletier, R. Bassel-Duby, A. Jayasuriya, B. N. Fields, and N. Sonenberg.** 1985. Identification of a new polypeptide coded by reovirus gene S1. J. Virol. **54:**720–725.
28. **Sherry, B.** 1998. Pathogenesis of reovirus myocarditis. Curr. Top. Microbiol. Immunol. **233:**51–66.
29. **Sherry, B., F. J. Schoen, E. Wenske, and B. N. Fields.** 1989. Derivation and characterization of an efficiently myocarditic reovirus variant. J. Virol. **63:**4840–4849.
30. **Thoresen, M., K. Haaland, E. M. Loberg, A. Whitelaw, F. Apricena, E. Hanko, and P. A. Steen.** 1996. A piglet survival model of posthypoxic encephalopathy. Pediatr. Res. **40:**738–748.
31. **Tyler, K. L.** 1998. Pathogenesis of reovirus infections of the central nervous system. Curr. Top. Microbiol. Immunol. **233:**93–124.
32. **Tyler, K. L., P. Clarke, R. L. DeBiasi, D. Kominsky, and G. J. Poggioli.** 2001. Reoviruses and the host cell. Trends Microbiol. **9:**560–564.
33. **Tyler, K. L., M. K. Squier, A. L. Brown, B. Pike, D. Willis, S. M. Oberhaus, T. S. Dermody, and J. J. Cohen.** 1996. Linkage between reovirus-induced apoptosis and inhibition of cellular DNA synthesis: role of the S1 and M2 genes. J. Virol. **70:**7984–7991.
34. **Tyler, K. L., M. K. Squier, S. E. Rodgers, B. E. Schneider, S. M. Oberhaus, T. A. Grdina, J. J. Cohen, and T. S. Dermody.** 1995. Differences in the capacity of reovirus strains to induce apoptosis are determined by the viral attachment protein sigma 1. J. Virol. **69:**6972–6979.
35. **Virgin, H. W., T. S. Dermody, and K. L. Tyler.** 1998. Cellular and humoral

immunity to reovirus infection, p. 147–162. *In* K. L. Tyler and M. B. A. Oldstone (ed.), Reoviruses II. Cytopathogenicity and pathogenesis. Springer-Verlag, New York, N.Y.

36. **Virgin, H. W., R. Bassel-Duby, B. N. Fields, and K. L. Tyler.** 1988. Antibody protects against lethal infection with the neurally spreading reovirus type 3 (Dearing). J. Virol. **62:**4594–4604.
37. **Weiner, H. L., D. Drayna, D. R. Averill, Jr., and B. N. Fields.** 1977. Molecular basis of reovirus virulence: role of the S1 gene. Proc. Natl. Acad. Sci. USA **74:**5744–5748.
38. **Weiner, H. L., M. L. Powers, and B. N. Fields.** 1980. Absolute linkage of virulence and central nervous system cell tropism of reoviruses to viral hemagglutinin. J. Infect. Dis. **141:**609–616.